J Mater Sci (2011) 46:896–901
DOI 10.1007/s10853-010-4832-6

Study on electrical transport and photoconductivity in iodine-doped cellulose fibers

A. S. Zakirov · Sh. U. Yuldashev · H. J. Wang · J. C. Lee · T. W. Kang · A. T. Mamadalimov

Received: 23 June 2010 / Accepted: 14 August 2010 / Published online: 8 September 2010

Abstract The electrical transport and photoconductivity of pure and iodine-doped cellulose fibers have been studied. The studies were conducted in the temperature range 293–363 K, while the electric field was varied over the range 1–100 V cm^{-1}. The conductivity of the iodine-doped cellulose fibers shows significant enhancement by more than four orders of magnitude as compared to undoped samples. The analysis reveals that the electrical conduction follows Ohm's law for iodine-doped samples, while for the undoped samples the bulk-limited Pool–Frenkel conduction mechanism is likely to dominate for the steady state current. Especially, the clear photoconduction response at UV and visible region indicates that photoconduction is essential due to band-to-band electron–hole pair's generation and that doped CF is a good conductor of photogenerated carriers.

Introduction

Electrical conduction in polymers has been studied extensively during the past two decades to understand the nature of charge transport in these materials [1–3]. The elucidation of the charge injection and carrier migration processes will become essential for the future use of these materials. The conduction mechanism is mainly characterized by the transport parameters, such as charge carrier density and charge carrier mobility. Considerable interest has been shown on the effect of doping on the transport properties of polymers [4–6]. Chemical, photochemical, or electrochemical doping is used to introduce extrinsic charge carriers into organic semiconductors [7–9]. Depending on their chemical structure and the way, in which they react with the macromolecular matrix, doping substances decrease the resistivity of the polymers to different degrees [10].

The natural cotton fibers offer wide possibilities in this regard. These cellulosic fibers (CFs) may be considered to be polycrystalline materials with much smaller particle size and relatively larger fraction of grain boundaries. Moreover, the CF is supposed to have different morphology with respect to processing conditions [11]. The reason for such a variation, even though these are made up of same chemical units, lies in the fact that the number of inter- and intra-weak hydrogen bonds like C–H···O, O–H···O, and N–H···O determines the extent of ordering in the CF [12]. As the processing conditions vary, the morphology of the resulting cellulose fibers may change. This will lead to the change in the physical properties of the resulting materials [13]. Many research groups have been studying these modifications using different approaches which include a variety of chemical treatments, grafting, couplings between fiber and matrix, and physical coverage of the fibers by a polymer sleeve [14]. Most studies have been focused on in situ polymerization to produce conductive cotton fabric since this method does not require the destruction of the substrate and provides reasonably good conductivity [15]. Its electrical conductivity and charge-storage capability can

A. S. Zakirov · Sh. U. Yuldashev · H. J. Wang · J. C. Lee · T. W. Kang (✉)
Quantum-Functional Semiconductor Research Center, Dongguk University, Seoul 100715, Republic of Korea
e-mail: twkang@dongguk.edu

A. S. Zakirov · Sh. U. Yuldashev
Department of Thermophysics, Academy of Sciences, Tashkent 100135, Uzbekistan

A. T. Mamadalimov
Department of Physics, National University of Uzbekistan, Tashkent 100175, Uzbekistan

be markedly influenced by doping of the physical covered cotton fabric with suitable impurities. These fabrics are used for industrial applications, such as filters, as well as home and business applications, including electrostatic dissipating and electromagnetic interference shielding. The microwave absorption characteristics of these fabrics are also highly desirable, thus allowing these materials to be used in military applications such as camouflage and radar protective fabrics for stealth technology. Although much progress has been made in studying to produce conductive fabric, understanding the relationship between charge transport, morphology, and chemical structure is still a big challenge. The mechanism of electrical transport in CFs is also of considerable interest in view of the number of possible technical applications of such fibers. To the best of our knowledge a photoconductivity of the iodine-doped CF has not been reported so far in the literature, thus no picture is available with respect to charge transport phenomena.

The present article reports the results of steady state conduction current measurements on alkali solution-treated pure and iodine-doped cotton fibers with metallic electrodes. The purpose of this study was to carry out a careful investigation of the steady state conduction in pure and doped CF elucidating, (i) the action of dopants molecules in modifying the conduction characteristics of the polymer matrix when they are doped in various concentrations, (ii) the mechanism of charge carrier transport which depends on both the temperature and electric field, and (iii) the effect of doping on the photophysical properties. It is known that, through chemical and/or mechanical iodine doping, polymeric materials can be generated with electrical conductivities that vary over a wide range from insulator to metallic like materials [16–18].

Experimental

Scouring of cotton

First, 1 g of raw cotton is weighed to prepare pure and doped fibers. Cotton should undergo washing before starting the operation for doping process. After washing, cotton fibers are placed in bath with 20% NaOH solution for 2 min at temperature below 15 °C. The product is removed out of the bath, rinsed at several times with water, and dried in standard conditions of 65% relative humidity at 20 °C. This operation leads to an increase in stability of cotton goods and absorption of reagents, and both these characteristics are effective in doping with conductive polymer processes. The isothermal immersion technique was utilized to prepare doped samples. Iodine was dissolved in ethanol at the 5% concentration. Mercerized fibers were immersed vertically into the solution for a period of 15 min. After the fibers were taken out and were annealed in the air at 70 °C for 6 h to reach the equilibrium state.

The specimens ($1.0 \times 0.5 \times 0.2$ cm^3) with silver electrodes were sandwiched between two tungsten electrodes of a special temperature chamber. The low current of nanoampere level I–V characteristics in the dark and upon UV illumination (at 254 nm) was measured under air using Keithley 617 electrometer. The measurements were carried out on metal–cotton and fiber–metal structure with current–voltage (I–V) and current–time (I (t)) methods in the temperature range 293–363 K and at electrical field range 1–100 V cm^{-1}, respectively. The temperature was measured using a copper constantan thermocouple in perfect contact with the specimen.

Results and discussion

Conductivity of the pure and doped samples

Current as a function of voltage and temperature has been studied in pure and iodine-doped cellulose fibers. Upon first applying a voltage across a pure CF, extremely small currents were obtained. The current never exceeded 10^{-9} A up to a voltage of 100 V. The conductivity was calculated by measuring the current flow through a piece of the sample as follows $\sigma = I\ (l/SV)$, where l (cm) is the sample length, S is its area (cm^2), V is the potential across the materials, and I is the observed steady state current. The specific electrical conductivity of the pure CF is found to be around $7.8 \times 10^{-10}\ \Omega^{-1}\ \text{cm}^{-1}$ at room temperature. The other form of conductivity can be expressed as [19] $\sigma = \Sigma\ q_i\ n_i\ \mu_i$, where n_i is the charge carrier density and μ_i is the charge carrier mobility. Inserting the values of the conductivity ($\sim 8 \times 10^{-10}\ \Omega^{-1}\ \text{cm}^{-1}$) and the average mobility ($\sim 10^{-3}\ \text{cm}^2\ \text{V}^{-1}\ \text{s}^{-1}$) [20] into the above equation, the number of the charge carrier contributing the electrical conduction in this bias range was found to be $n_0 \sim 10^{10}\ \text{cm}^{-3}$. Given the large energy gap of about 3.3 eV, a low value n_0 is understandable. In contrary, the steady state current values for doped samples are higher than those found for pure CF at the same operating temperatures and electrical fields. The conductivity of the fibers increased on doping with iodine by more than four orders of magnitude and was found to be $5.6 \times 10^{-6}\ \Omega^{-1}\ \text{cm}^{-1}$ at room temperature. Thus, the number of the calculated charge carriers was also increased from $\sim 10^{10}\text{cm}^{-3}$ to $\sim 10^{14}\ \text{cm}^{-3}$. The conductivity increasing can be explained as follows. When dopants molecules are present they will start bridging the gap separating the two localized sites and lowering the potential barrier between them, thereby facilitating the transfer

of charge carriers between two localized states. This behavior may occur because charge transfer complexes are formed in the polymer effectively decreases the trapping effects by "handing on" the carriers. From this, we can be deduced that the conduction enhancement with increasing electrical field is apparently due to the gradual increase of bulk generated free carrier density.

Temperature–current characteristics

To better understand the conduction mechanism of cellulose fibers, we have performed the two-point probe conductivity measurement on pure and doped samples during heating and cooling cycles between room temperature and 363 K. Figure 1 shows the current at 100 V obtained from a pure sample as a function of temperature. The current versus $10^3/T$ has been plotted for the both CF samples to evaluate the activation energies (Fig. 1). It can be seen that the current at a given voltage increased with increasing temperature and characterized by two slopes. In the low temperature region below 323 K, there is a slight change in conductivity, while in the high temperature region there is a rapid change in conductivity. Since there is a positive temperature coefficient of electric conductivity for both regions, the samples have a semiconducting character. This phenomenon has also been observed for cotton fabrics by several other research groups [21, 22]. Cellulosic materials are excellent electrical insulators when dry, contain a large number of traps and exhibit structural deformations at certain transition temperatures [13]. Therefore, the complex morphology of the conducting polymers has made it difficult to determine the intrinsic conductive behavior. Consequently, the exponential relationship between the conductivity and temperature is related to the charge carrier generation, not only due to the intrinsic band transition, but also to some other thermally activated processes. The conductivity behavior of such fibers may be dominated by the properties of the amorphous regions, the presence of which gives rise to localized states. The fact that mercerized CFs are considered as mixed crystalline (cellulose I or cellulose II) and/or an amorphous cellulosic phase, the increase in conductivity at high temperatures may be attributed to the liberation of electrons or ions through the amorphous regions of polymeric materials. Bailey et.al [23] showed that the onset of molecular motion increases the conductivity of the polymer by helping the charge carriers to escape from and transport to localized states such as surface and bulk dipole states, molecular ion states, impurities, chain ends and branches, and crystalline-amorphous boundaries. In our view, the existence of two activation energies could plausibly be correlated with the presence of mixed crystalline (cellulose I or cellulose II) and/or an amorphous cellulosic phase. The electrical transport is, therefore, likely to be influenced by the potential barrier and in homogeneities due to the grain boundaries.

From Fig. 1 (inset), it can be seen that upon iodine doping the general trend of the conductivity–temperature dependence is similar, i.e., curves have the same positive temperature activated behavior, like in undoped CF. The room temperature conductivity of doped samples before and after temperature dependent measurements remains essentially unchanged, which shows clearly that annealed samples are very close to the equilibrium state and exhibit good air stability at elevated temperatures. The obtained activation energies in the temperature range (50–100 °C) were found to be 0.68 eV for the pure CF and 1.03 eV for the doped samples in the same temperature range, respectively. It indicates that at high doping level the I_2 molecules induces the additional disorder and the high concentration of hopping centers are created. The dopant molecules are considered to act as additional trapping centers and provide links between the polymer molecules in the amorphous region, thus resulting in the formation of charge transfer complexes. Because there are many localized states, the release or excitation of the carriers in these states dominates the conduction process. According to Dwyer [24], there exist shallow traps of low energy range and deep traps of higher energy range in the samples. The shallow traps exist below the continuum of free levels, while deep traps lie between conduction and valence bands. At sufficiently low temperatures, electrons are trapped deeply, but with increasing the temperature they get excited and leave the deep traps to enter into the shallow traps or conduction band and take part in the process of conduction under the influence of the applied field. The low values of activation energy for the investigated samples (0.68 eV) [25] are usually indicative of the predominance of electronic

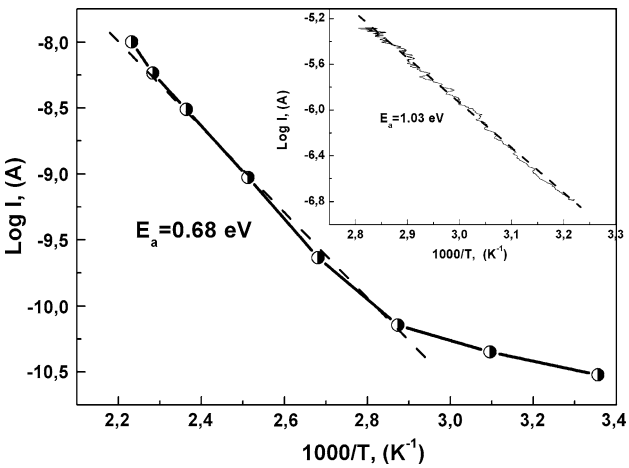

Fig. 1 Arrhenius plot for leakage current versus temperature for the undoped and (inset) iodine-doped CF

conduction, while higher values at lower temperature point to the participation of ionic conduction.

Current–voltage characteristics

The current flowing through the undoped and doped samples as a function of applied voltage was measured while maintaining the sample at constant temperatures of RT. During the leakage current–voltage measurement, it was observed that the leakage current decreased about 5–7% with time after first applying the voltage, particularly for a leakage current level $\sim 10^{-10}$ A. A higher electric field gives a shorter time to reach the steady state current. This change in time dependence suggests the initial and later current are due to different conduction mechanisms. The temporal decay of the currents is probably due to absorption current caused by the dipole orientation, electron traps in the bulk of the sample, and charge accumulation in the vicinity of the electrode or ionic conduction, caused by internal charge drifts, resulting in a decrease of the effective electric field in the bulk of the sample [19]. Because relaxation time is usually independent of electric field, the observed decay is, therefore, not due to the dipole orientation. On the other hand, the ionic conduction also will not be considered is due to that charge transport requires mass transport, the supply of carriers is depleted and the current density must be observed to decrease rapidly as several coulombs are passed through the sample. Therefore, we look beyond dipole orientation and ionic conduction for the origin of the charge carriers for the pure and doped CF, such as electrode effects (Schottky effects) or bulk effects (Pool–Frenkel).

The isothermal log *I*–*V* plot, at room temperature, for the undoped and doped samples is shown in Fig. 2 and inset, respectively. Two slopes are observed for the undoped sample. The plots show a linear behavior with appreciable deviation from linearity at lower fields. In this case, the slope value at low field is around 0.6, but at high fields, is about 0.85. This indicates that the current–voltage relationship is non-ohmic in all investigated region. After doping (Fig. 2, inset), the log *I*–*V* plot displays on Ohmic behavior (the slope is ~ 1) and increases linearly with *V*, being consistent with results reported by other groups. For the both samples these results cannot be explained on the basis of space-charge limited current, as the slope for this type of mechanism is around 2 [26]. The other possible mechanisms are (a) charge carrier injection into the film from the contact via field-assisted lowering of the metal–insulator potential barrier, i.e., Schottky-Richardson (SR) emission, and (b) release of charge carriers from traps via field-assisted lowering of trap depth, i.e., Poole–Frenkel (PF) effect. The current–voltage relationship for SR emission is given by [26]

$$I = A * T^2 \exp\left(-\Phi s/kT + \beta_{SR} V^{1/2}\right) \quad (1)$$

where, A^* is the effective Richardson constant, $\beta_{SR} = (1/kT)\left(e^3/4\pi\varepsilon_0\varepsilon d\right)^{1/2}$ is Schottky-field lowering constant, Φs is the metal electrode-insulator potential barrier, *T* is temperature, *K* is Boltzmann's constant, ε_0 is the permittivity of free space, ε is the high-frequency dielectric constant of the material, *d* is the length of the sample, and *V* is applied voltage. Equation (1) predicts a linear relationship between log *I* and $V^{1/2}$ with a slope β_{SR} at a constant temperature. The PF bulk-limited process also predicts a linear relationship between log *I* and $V^{1/2}$ similar to Eq. (1) with β_{SR} replaced by β_{PF} and Φs replaced by Φ_{PF}—which is trap depth. Theoretically, $\beta_{PF} = 2\ \beta_{SR}$.

The log *I* versus $V^{1/2}$ for the undoped and doped CF is shown in Fig. 3 and inset, respectively. The results for high

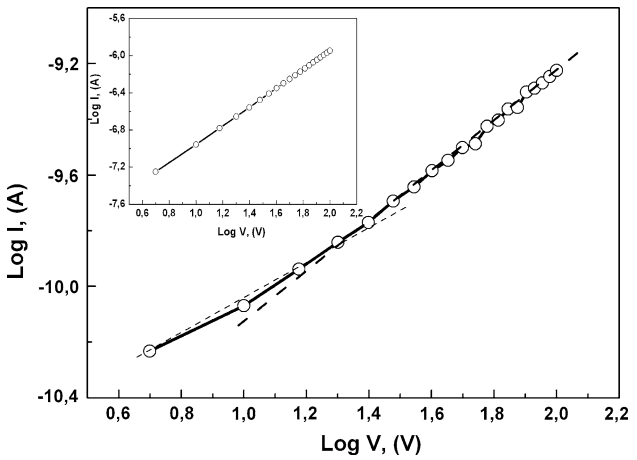

Fig. 2 Voltage dependence of leakage current in the form of a log *I*–*V* plot for the undoped and (inset) iodine-doped CF

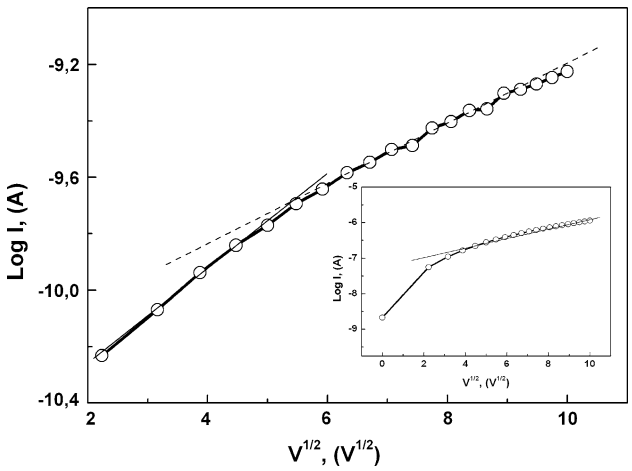

Fig. 3 The log *I* as function of $V^{1/2}$ for undoped and (*inset*) iodine-doped CF

Table 1 Theoretical and experimental values of β for undoped and I_2-doped cellulose fibers

Sample	β_{SR} (experimental)	β_{PF} (experimental)	β (theoretical)
Undoped CF	0.114	0.228	0.222
I_2-doped CF	0.124	0.248	

fields are reasonably well represented by straight lines, while the data for low fields deviate from the straight line. Moreover, the slope value of log I versus $V^{1/2}$ at lower voltages (i.e., the deviated straight line) for the doped sample is higher than that for the undoped sample. The higher value of the slope at lower voltages can be explained on the basis of space-charge buildup at the electrode, which enhances the field at the electrode and leads to the high slope of the log I–$V^{1/2}$ curve. This suggests that the charge carrier generation is basically from the electrodes which are indicative of SR mechanism. At higher voltages, charge carriers injected by lowering the electrode-insulator potential barrier because of which the field at the electrode is reduced, and the slope of the log I–$V^{1/2}$ plot approaches the theoretical value. At higher voltages, the linear behavior of log I–$V^{1/2}$ plot in this study points to an electronic-type conduction mechanism. In order to differentiate between SR emission and PF effect, the values of β were calculated from the slopes of log I–$V^{1/2}$ plots, and the experimental as well as the theoretical values of β are shown in Table 1. For undoped films, the experimental value of β_{exp} is closer to the theoretical value of β_{PF}. This suggests that the charge conduction is through the Poole–Frenkel mechanism. In this case, the emitted current is due to the thermal excitation of trapped electrons into the conduction band which is enhanced by an external field. In polymers, surface states, chain folding, molecular disorders, crystalline-amorphous boundaries, and chain ends may act as trapping sites. In addition, many polymers contain polar groups where each dipole can act as an electron or hole trap. The charge carriers trapped at these sites may be excited and contribute to the total conduction. In fact, this type of mechanism has also been observed in other types of polymers [19, 26].

Charge separation effects in the photoconductivity

The I–V characteristics in the dark and upon UV illumination were measured under air using 30 W halogen lamp as light source. Figure 4 shows fully-ohmic I–V characteristic curves of the CF measured in the dark (1) and under UV illumination (2), at RT. The measured average dark current of the CF linearly increased to 0.1 μA as the bias increased from 0 to 10 V. Upon UV illumination (254 nm),

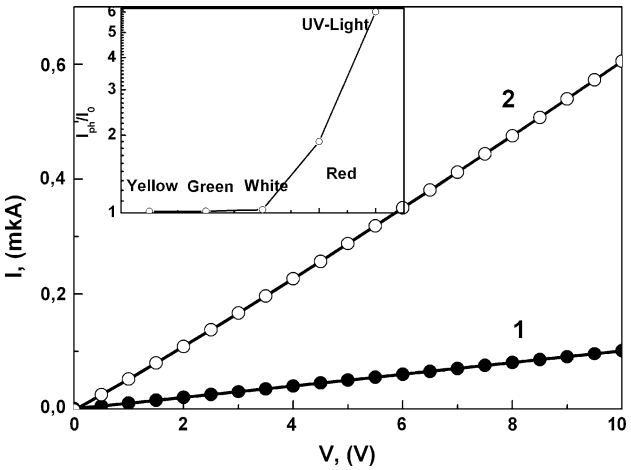

Fig. 4 Dark and photocurrent versus forward bias voltage for iodine-doped CF under UV light (maximum intensity at 254 nm) illumination. Inset: Photoresponse of the iodine-doped samples under different light illuminations

the photocurrent (PC) jumped to 0.62 μA at 10 V bias, indicating a photosensitivity and photocurrent to dark current ratio of 6. To stimulate the photoresponse in doped CF, we used a set of LEDs at different energies from UV to visible range. As seen in Fig. 4, inset under white, yellow, and green light illuminations, PC increases less than 5–7%, while for red and UV illumination, the photoresponse is about 21 and 500%, respectively. Fundamental (band-to-band absorption) takes place in the UV. This indicates that photoconduction is essentially due to band-to-band electron–hole pair's generation. From the technological point of view, these results also suggest that doped CF is UV photodetectors with response in the UV and visible region. For the undoped samples, typical conductance values were always below 0.1 nS, and any significant photoresponse was observed after UV illumination. The present observation of enhancement of photoconductivity in CF upon iodine doping can be explained by the photo-induced charge transfer between I_2 molecules and the polymeric network [27]. Such a tendency is unique to organic polymers and could be related to the carrier generation and exciton diffusion processes as well as the charge separation processes. As discussed by Cheng et al. [28], the improvement of the charge generation efficiency rather than carrier transport is believed to be the dominant factor in the enhancement of the photoconductivity. Moreover, Khare [9] reported that the percentage of UV absorption of the doped cellulose films becomes higher than that of the undoped films, increasing with increase of the dopant concentration. This suggests that the electron transfer from CF to iodine is energetically favorable in the ground state, which is consistent with the increasing of the absorption spectrum and the electrical conductivity in CF by iodine

doping. Hence, upon illumination by visible light, generation of free charge carriers takes place mainly inside the organic matrix. The doping effect of iodine depends on the appearance of the photoresponse at red illumination region, can be interpreted due to photoexcitation of electrons from the ground state of iodine to the excited state and followed hole tunneling into the CF chain. Especially, the clear photoconduction response at 2.0 eV indicates that doped CF is a good conductor for photogenerated carriers.

Conclusions

In conclusion, the electrical conduction current of pure and doped CF fibers is measured as function of time, electric field, and sample temperature. The experimental results were analyzed and fitted to the theoretical curves for several conduction mechanisms. We found that the conductivity of the fibers increased on doping with iodine by more than four orders of magnitude, and the Ohmic conduction mechanism is likely to dominate for the steady state current. The observed substantial conductivity enhancement in iodine-doped CF can be attributed to two factors: the higher conductivity of doped CF due to the increased number of the charge carriers and the gradual increase of bulk generated free carrier density. The dopant molecules are considered to act as additional trapping centers and provide links between the polymer molecules in the amorphous region, thus resulting in the formation of charge transfer complexes. Comparing the experimental as well as the theoretical values of β for both the Schottky and Poole–Frenkel mechanisms we have found that for the undoped polymer fibers, the Poole-Frencel mechanism is the main conduction mechanism. Especially, the clear photoconduction response at UV and visible region indicates that photoconduction is essentially due to band-to-band electron–hole pair's generation and explained by the photo-induced charge transfer between I_2 molecules and the polymeric network.

Acknowledgements This study was supported by the National Research Foundation of Korea (NRF) grants funded by the Korea government (MEST) (No. K20901000002-09E0100-00210, No. 2010-0000751) and by the Fundamental Research Foundation of Uzbekistan (Grant No. OT-F2-084).

References

1. Kuhn HH, Kimbrell WC, Fowler JE, Barry CN (1993) Synth Met 57:3707
2. Günes S, Neugebauer H, Sariciftci NS (2007) Chem Rev 107:1324
3. Abd El-kader FH, Osman WH, Ragab HS, Shehap AM, Rizk MS, Basha MAF (2004) J Polym Mater 21:49
4. Sarada H, Sawamura K, Yoda K (1971) Polym J 2:518
5. Mort J, Pfister G (1979) Polym Plast Technol Eng 12:89
6. Gill WD (1972) J Appl Phys 43:5033
7. Khare PK, Chandok RS (1995) Phys Status Solidi 147:509
8. Lekpittaya P, Yanumet N, Grady BP, O'Rear EA (2004) J Appl Polym Sci 92:2629
9. Khare PK, Upadhayay JK, Verma A, Paliwal SK (1998) Polym Int 47:145
10. Aleshin AN (2006) Adv Mater 18:17
11. Hon DN-S (1994) Cellulose 1:1
12. Abhishek S, Samir OM, Annadurai V, Gopalkrishne Urs R, Mahesh SS, Somashekar R (2005) Eur Polym J 41:2916
13. Cunha AG, Freire CSR, Silvestre AJD, Neto CP, Gandini A, Orblin E, Fardim P (2007) Langmuir 23:10801
14. Boufi S, Gandini A (2001) Cellulose 8:302
15. Oh KW, Hong KH, Kim SH (1999) J Appl Polym Sci 74:2094
16. Park JG, Kim GT, Krstic V, Lee SH, Kim B, Roth S, Burghard M, Park YW (2003) Synth Met 119:469
17. Kaiser AB, Park JG, Kim B, Lee SH, Park YW (2004) Curr Appl Phys 4:497
18. Kaiser AB, Park YW (2002) Curr Appl Phys 2:33
19. Lee K, Murarka SP (1998) J Mater Sci 33:4105. doi: 10.1023/A:1004480531373
20. Redecker M, Bradley DDC, Inbasekaran M, Wu WW, Woo EP (1999) Adv Mater 11:241
21. Abou-Sekkina MN, Saafan AA, Sarkan MA, Ewaida MA (1986) J Therm Anal 31:791
22. Saran MA (1996) J Radioanal Nucl Chem Lett 213:51
23. Bailey RT, North AM, Pethrick RA (1981) Molecular motion in high polymers. Oxford, New York
24. Dwyer OJJ (1966) J Appl Phys 37:2599
25. Abd El-kader FH, Gaafer SA, Mahmoud KH, Mohamed SI, Abd El-kader MFH (2009) Polym Compos 17:214
26. Sekar R, Tripathi AK, Goel TC, Pillai PKC (1987) J Appl Phys 62:4196
27. Morita S, Kiyomatsu S, Yin XH, Zakhidov AA, Noguchi T, Ohnishi T, Yoshino K (1993) J Appl Phys 74:2860
28. Cheng J, Wang S, Li XY, Yan YJ, Yang S, Yang CL, Wang JN, Ge WK (2001) Chem Phys Lett 333:375